Table III. Correlation coefficient between MPO-ANCA ELISAs.

MPO-ANCA ELISAs	Nipro	MBL [BS]	Wieslab
Nipro	–	0.891	0.879
MBL	0.891	–	0.899
Wieslab	0.879	0.899	–

Samples with PSV before treatment and in the follow up period (n=146).

Table IV. Percentage of ANCA positivity in PSV patients.

	Diagnosis / ELISA positivity	MPA % (n)	WG % (n)	CSS % (n)
Nipro	MPO-ANCA	86.5 (45/52)	0 (0/11)	0 (0/1)
	PR3-ANCA	3.8 (2/52)	100.0 (11/11)	0 (0/1)
	Double positive	1.9 (1/52)	0 (0/11)	0 (0/1)
	Double negative	7.7 (4/52)	0 (0/11)	100.0 (1/1)
MBL	MPO-ANCA	80.8 (42/52)	0 (0/11)	100.0 (1/1)
	PR3-ANCA	7.7 (4/52)	100.0 (11/11)	0 (0/1)
	Double positive	3.8 (2/52)	0 (0/11)	0 (0/1)
	Double negative	7.7 (4/52)	0 (0/11)	0 (0/1)
Wieslab	MPO-ANCA	82.7 (43/52)	0 (0/11)	0 (0/1)
	PR3-ANCA	3.8 (2/52)	90.9 (10/11)	0 (0/1)
	Double positive	3.8 (2/52)	0 (0/11)	0 (0/1)
	Double negative	9.6 (5/52)	9.1 (1/11)	100.0 (1/1)

Double positive, both MPO- and PR3-ANCA positive;
Double negative, both MPO- and PR3-ANCA negative;
MPA: microscopic polyangiitis; WG: Wegener's granulomatosis;
CSS: Churg-Strauss syndrome.

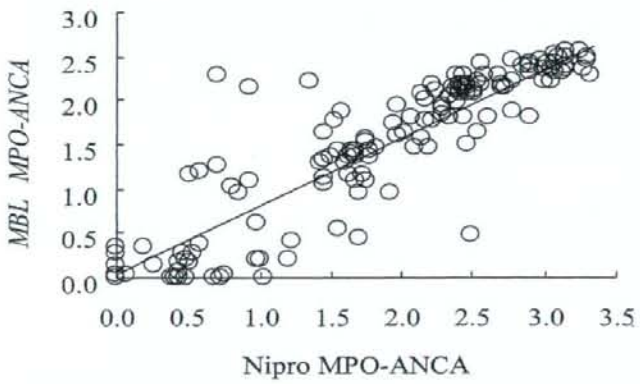

Fig. 1. *Correlation between Nipro MPO-ANCA and MBL MPO-ANCA.* Correlations between MPO-ANCA were analysed using 146 plasma samples from patients with PSV in the active and follow-up stages (MPA, n=132; CSS, n=1; WG, n=13). Nipro MPO-ANCA and MBL MPO-ANCA positively correlated with each other ($r = 0.891$, $p<0.0001$). *Estimated Nipro MPO-ANCA* = 1.0146×MBL MPO-ANCA + 0.3545, *Estimated MBL MPO-ANCA* = 0.7829 ×Nipro MPO-ANC II + 0.0265. All data were $\log_{10}$ transformed to normalise distributions prior to these analyses.

Clinical diagnostic performance of IIF for PSV.

Plasma samples of untreated PSV patients (n=64), disease controls (n=54), and healthy controls (n=55) were tested for positivity of IIF-ANCA. IIF showed a sensitivity of 81.3% (95% CI, 69.5–89.9) and 94.5% specificity (88.4–97.9) for active PSV.

P-ANCA and C-ANCA were detected in 46 and 11 out of the total 173 samples. Among the 57 samples with positive P- or C-ANCA by IIF, 56 samples were positive for MPO- and/or PR3-ANCA by Nipro MPO- and PR3-ANCA ELISAs. All the 57 samples with positive P- or C-ANCA were positive for MPO- and/or PR3-ANCA by MBL MPO- and PR3-ANCA ELISAs. The result of ELISAs by Nipro and MBL were well corresponded with ANCA by IIF. P-ANCA positivity in MPA was 82.7% (43/52), while C-ANCA positivity in MPA was 7.7% (4/52). Absence of P- and C-ANCA in MPA was 9.6% (5/52). C-ANCA and P-ANCA positivity in WG is 54.5% (6/11) and 9.1% (1/11) respectively. Absence of P- and C-ANCA in WG was 36.4% (4/11). IIF-ANCA was negative in our CSS patient (Table V).

Discussion

In this study we investigated ANCA ELISA systems authorized by the Japanese Ministry of Health and Welfare for diagnostic purpose: a streptavidin coated capture ELISA and a direct ELISA for MPO-ANCA and direct ELISAs for PR3-ANCA.

The present study shows that the ELISA systems widely used in Japan are highly sensitive and specific for detection of MPO-ANCA in MPA. There were no detectable differences in diagnostic performance between ELISA systems as analysed by ROC curve analysis.

The incidence of WG among the ANCA-associated systemic vasculitides is higher than MPA in northern Europe (10-13). By contrast, nationwide Japanese surveys demonstrated that the prevalence of patients with WG is very low compared with that of patients with MPA (14). Fujimoto *et al.* shows that the estimated annual incidence of MPA in Miyazaki Prefecture, the Southern part of Japan, is 14.8/million, which is as frequent as that of ANCA-associated systemic vasculitides identified in several European studies. They also demonstrate that MPA are more common than WG among the ANCA-associated vasculitides in Japan (15). MPO-ANCA was identified in 79 to 93% of patients with MPA in Japan, whereas reports from Europe described the ratio as being 44 to 69% (12-19).

Table V. Percentage of indirect immunofluorescence (IIF) test positivity in primary systemic vasculitis patients.

Diagnosis IIF positivity	MPA % (n)	WG % (n)	CSS % (n)
P-ANCA	82.7 (43/52)	9.1 (1/11)	0 (0/1)
C-ANCA	7.7 (4/52)	54.5 (6/11)	0 (0/1)
Negative	9.6 (5/52)	36.4 (4/11)	100 (1/1)

P-ANCA: perinuclear ANCA; C-ANCA: cytoplasmic ANCA;
Negative: both P- and C-ANCA negative.

Although differences in several clinico-epidemiological manifestations among vasculitides have been identified between Japan and European countries, it was suspected that such difference may result from different ELISA systems employed in Japan and Europe. However, this study shows MPO-ANCA predominance in Japan is not due to the different ELISA system employed in Japan and Europe. Therefore, the ANCA-associated systemic vasculitides epidemiologically and serologically differ between Japan and European countries.

Nevertheless, we should still bear in mind that there are significant differences in sensitivity and specificity among commercially available ELISA systems (3, 20-25). The reason might be that in ELISAs, proteins are denatured during antigen purification or coating onto the solid phase, thereby hiding or destroying conformational epitopes on PR3 or MPO. In order to avoid this, capture ELISA in which the plate is pre-coated with a monoclonal antibody to capture the antigen has been designed. Csernok *et al.* reported that capture PR3 ELISA was a highly sensitive assay in WG in several international laboratories (23). Recently Hellmich *et al.* reported sensitivity of a new anchor PR3-ELISA for WG was superior to those of usual direct or capture PR3-ELISA. They used a new technique to immobilize PR3 on the ELISA plate by using a bridging molecule as an "anchor" preventing direct adhesion to the plastic surface and thereby preserving all epitopes for binding with ANCA (24).

Another important issue is that the lack of the standard sera and international unit makes it difficult to compare ELISAs from different manufacturers. For example, Nipro MPO-ANCA and MBL MPO-ANCA are widely used in reference laboratories or university hospitals in Japan. Although sensitivity and specificity were not different between these two systems and they were positively correlated with each other (Fig. 1, Table III), the absolute values obtained from these two ELISA systems cannot be compared because they do not use the same standard serum.

We should also discuss cut-off values employed in the ELISA systems. Holle *et al.* analysed ANCA ELISAs from 11 manufacturers and reported that applying the manufacturers' cut off values results in great variation in sensitivity. Lowering the cut off values increased the sensitivity and reduced specificity but increased overall diagnostic performance (3). They concluded that the low sensitivity of some commercial ELISA systems reflects the high cut off values rather than methodological problems in the assays.

For standardization of ANCA testing, the BCR office of the European Union sponsored a large international standardization project of monitoring different antigen purification methods (26), suitability of purified antigens for solid-phase assays and standardization (27), and clinical utility of the developed tests (28). In the meantime, before the results become clear, it is important that laboratories should understand the difference and limitations of the assays in use.

A limitation of our study is the small number of WG samples. It was difficult to collect samples from patients with active and untreated WG because MPA with renal involvement predominates in Japan but we do not see patients with WG presenting to renal units. Therefore the PR3-ANCA ELISA kit available in Japan is not manufactured in Japan. Nipro PR3-ANCA is equivalent to Immunoscan PR3-ANCA (Euro-Diagnostica) and MBL PR3-ANCA is equivalent to BINDAZYME™ Human Anti-PR3 Enzyme Immunoassay kit (Binding Site). These kits are used internationally and already well screened in the world. Trevisin *et al.* reported that sensitivity of Euro-Diagnostica Immunoscan PR3-ANCA was 90% sensitivity and 96% specificity (25). Binding Site BINDAZYME RP3-ANCA ELISA were reported 60-96% sensitivity and 88-100% specificity. (3, 25, 29). Further study should be required to investigate the performance of the ELISA systems using larger samples from Japanese patients with active and untreated WG. Then, it would be possible to more directly compare the performance of ELISAs for WG between Europe and Japan.

Another limitation is that we used plasma and not serum samples. However, Lee *et al.* reported that ANCA positivity between serum and plasma as measured by commercially available ELISA systems was concordant, and that ANCA levels in serum and plasma measured by solid phase assays correlated well (30). Therefore, our results could be compared with those tested with serum samples.

In summary, the two major MPO-ANCA ELISA systems commercially available in Japan exhibited high sensitivity and specificity that provided similar diagnostic value with the ELISA systems used in Europe. Thus, the results of ANCA testing in Japan may be compared to those from other countries. This will facilitate future international surveys exploring differences in the epidemiology of PSV, and aetiological factors contributing to their pathogenesis.

Acknowledgements

The authors thank Dr. Katsumi Yagi, Louis Pasteur Center for Medical Research, for advices in statistical analysis and Dr. Masato Yagita, Department of Clinical Immunology and Rheumatology, Tazuke Kofukai Medical Research Institute, Kitano Hospital, for providing patient blood samples for analysis.

References

1. SAVIGE J, GILLIS D, BENSON E *et al.*: International Consensus Statement on Testing and Reporting of Antineutrophil Cytoplasmic Antibodies (ANCA). *Am J Clin Pathol* 1999; 111: 507-13.
2. SAVIGE J, DIMECH W, FRITZLER M *et al.*: Addendum to the International Consensus Statement on testing and reporting of antineutrophil cytoplasmic antibodies. Quality control guidelines, comments, and recommendations for testing in other autoimmune diseases. *Am J Clin Pathol* 2003; 120: 312-8.
3. HOLLE JU, HELLMICH B, BACKES M *et al.*: Variations in performance characteristics of commercial enzyme immunoassay kits for detection of antineutrophil cytoplasmic antibodies: what is the optimal cut off? *Ann Rheum Dis* 2005; 64: 1773-9.
4. LEAVITT RY, FAUCI AS, BLOCH DA *et al.*: The American College of Rheumatology 1990 criteria for the classification of Wegener's granulomatosis. *Arthritis Rheum* 1990; 33: 1101-7.
5. MASI AT, HUNDER GG, LIE JT *et al.*: The American College of Rheumatology 1990 criteria for the classification of Churg-Strauss syndrome (allergic granulomatosis and angiitis). *Arthritis Rheum* 1990; 33: 1094-100.
6. JENNETTE JC, FALK RJ, ANDRASSY K *et al.*: Nomenclature of systemic vasculitides. Proposal of an international consensus conference. *Arthritis Rheum* 1994; 37: 187-92.
7. WATTS R, LANE S, HANSLIK T *et al.*: Development and validation of a consensus methodology for the classification of the ANCA-associated vasculitides and polyarteritis nodosa for epidemiological studies. *Ann Rheum Dis* 2007; 66: 222-7.
8. LUQMANI RA, BACON PA, MOOTS RJ *et al.*: Birmingham Vasculitis Activity Score (BVAS) in systemic necrotizing vasculitis. *QJM* 1994; 87: 671-8.
9. HANLEY JA, MCNEIL BJ: The meaning and use of the area under a receiver operating characteristic (ROC) curve. *Radiology* 1982; 143: 29-36.
10. HAUGEBERG G, BIE R, BENDVOLD A *et al.*: Primary vasculitis in a Norwegian community hospital: a retrospective study. *Clin Rheumatol* 1998; 17: 364-8.
11. WATTS RA, LANE SE, BENTHAM G *et al.*: Epidemiology of systemic vasculitis: a ten-year study in the United Kingdom. *Arthritis Rheum* 2000; 43: 414-9.
12. LANE SE, SCOTT DG, HEATON A *et al.*: Primary renal vasculitis in Norfolk-increasing incidence or increasing recognition? *Nephrol Dial Transplant* 2000; 15: 23-7.
13. REINHOLD-KELLER E, HERLYN K, WAGNER-BASTMEYER R *et al.*: Stable incidence of primary systemic vasculitides over five years: Results from German vasculitis register. *Arthritis Rheum* 2005; 53: 93-9.
14. SAKAI H, KUROKAWA K, KOYAMA A *et al.*: [Guidelines for the management of rapidly progressive glomerulonephritis] *Nippon Jinzo Gakkai Shi* 2002; 44: 55-82.(in Japanese)
15. FUJIMOTO S, UEZONO S, HISANAGA S *et al.*: Incidence of ANCA-associated primary renal vasculitis in the Miyazaki prefecture: the first population-based retrospective, epidemiologic survey in Japan. *Clin J Am Soc Nephrol* 2006; 1: 1016-22.
16. GONZALEZ-GAY MA, GARCIA-PORRUA C, GUERRERO J *et al.*: The epidemiology of the systemic vasculitides in northwest Spain: Implications of the Chapel Hill Consensus Conference Definitions. *Arthritis Rheum* 2003; 49: 388-93.
17. TIDMAN M, OLANDER R, SVALANDER C *et al.*: Patients hospitalized because of small vessel vasculitides with renal involvement in the period 1975-1995: organ involvement, ANCA patterns, seasonal attack rates and fluctuation of annual frequencies. *J Intern Med* 1998; 244: 133-41.
18. HAUER HA, BAJEMA IM, VAN HOUWELINGEN HC *et al.*: Renal histology in ANCA-associated vasculitis: Differences between diagnostic and serologic subgroups. *Kidney Int* 2002; 61: 80-9.
19. FRANSSEN CF, STEGEMAN CA, KALLENBERG CG *et al.*: Antiproteinase 3- and antimyeloperoxidase-associated vasculitis. *Kidney Int.* 2000; 57: 2195-206.
20. SPECKS U, WIEGERT EM, HOMBURGER HA: Human mast cells expressing recombinant proteinase 3 (PR3) as substrate for clinical testing for anti-neutrophil cytoplasmic antibodies (ANCA). *Clin Exp Immunol* 1997; 109: 286-95.
21. LIM LC, TAYLOR JG 3RD, SCHMITZ JL *et al.*: Diagnostic usefulness of antineutrophil cytoplasmic autoantibody serology. Comparative evaluation of commercial indirect fluorescent antibody kits and enzyme immunoassay kits. *Am J Clin Pathol* 1999; 111: 363-9.
22. CSERNOK E, AHLQUIST D, ULLRICH S *et al.*: A critical evaluation of commercial immunoassays for antineutrophil cytoplasmic antibodies directed against proteinase 3 and myeloperoxidase in Wegener's granulomatosis and microscopic polyangiitis. *Rheumatology* (Oxford) 2002; 41: 1313-7.
23. CSERNOK E, HOLLE J, HELLMICH B *et al.*: Evaluation of capture ELISA for detection of antineutrophil cytoplasmic antibodies directed against proteinase 3 in Wegener's granulomatosis: first results from a multicentre study. *Rheumatology* (Oxford) 2004; 43: 174-80.
24. HELLMICH B, CSERNOK E, FREDENHAGEN G *et al.*: A novel high sensitivity ELISA for detection of antineutrophil cytoplasm antibodies against proteinase-3. *Clin Exp Rheumatol* 2007; 25: S1-5.
25. TREVISIN M, POLLOCK W, DIMECH W *et al.*: Antigen-Specific ANCA ELISAs Have Different Sensitivities for Active and Treated Vasculitis and for Nonvasculitic Disease. *Am J Clin Pathol* 2008; 129: 42-53.
26. HAGEN EC, ANDRASSY K, CHERNOK E *et al.*: The value of indirect immunofluorescence and solid phase techniques for ANCA detection. A report on the first phase of an international cooperative study on the standardization of ANCA assays. EEC/BCR Group for ANCA Assay Standardization. *J Immunol Methods* 1993; 159: 1-16.
27. HAGEN EC, ANDRASSY K, CSERNOK E *et al.*: Development and standardization of solid phase assays for the detection of anti-neutrophil cytoplasmic antibodies (ANCA). A report on the second phase of an international cooperative study on the standardization of ANCA assays. *J Immunol Methods* 1996; 196: 1-15.
28. HAGEN EC, DAHA MR, HERMANS J *et al.*: Diagnostic value of standardized assays for anti-neutrophil cytoplasmic antibodies in idiopathic systemic vasculitis. EC/BCR Project for ANCA Assay Standardization. *Kidney Int* 1998; 53: 743-53.
29. POLLOCK W, DUNSTER K, ROLLAND JM *et al.*: A comparison of commercial and in-house ELISAs for antineutrophil cytoplasmic antibodies directed against proteinase 3 and myeloperoxidase. *Pathology* 1999; 31: 38-43.
30. LEE AS, FINKIELMAN JD, PEIKERT T *et al.*: Agreement of anti-neutrophil cytoplasmic antibody measurements obtained from serum and plasma. *Clin Exp Immunol* 2006; 146: 15-20.

Expression of BMP-7 and USAG-1 (a BMP antagonist) in kidney development and injury

M Tanaka[1], S Endo[1], T Okuda[2], AN Economides[3], DM Valenzuela[3], AJ Murphy[3], E Robertson[4], T Sakurai[5], A Fukatsu[6], GD Yancopoulos[3], T Kita[1] and M Yanagita[2]

[1]Department of Cardiovascular Medicine, Graduate School of Medicine, Kyoto University, Kyoto, Japan; [2]COE Formation for Genomic Analysis of Disease Model Animals with Multiple Genetic Alterations, Graduate School of Medicine, Kyoto University, Kyoto, Japan; [3]Regeneron Pharmaceuticals Inc., Tarrytown, New York, USA; [4]Wellcome Trust Center for Human Genetics, University of Oxford, Oxford, UK; [5]Department of Pharmacology, Institute of Basic Medical Sciences, University of Tsukuba, Ibaraki, Japan and [6]Department of Artificial Kidneys, Graduate School of Medicine, Kyoto University, Kyoto, Japan

Once developed, end-stage renal disease cannot be reversed by any current therapy. Bone morphogenetic protein-7 (BMP-7), however, is a possible treatment for reversing end-stage renal disease. Previously, we showed that the BMP antagonist uterine sensitization-associated gene-1 (USAG-1, also known as ectodin and sclerostin domain-containing 1) negatively regulates the renoprotective action of BMP-7. Here, we show that the ratio between USAG-1 and BMP-7 expression increased dramatically in the later stage of kidney development, with USAG-1 expression overlapping BMP-7 only in differentiated distal tubules. Examination of USAG-1 expression in developing kidney indicated that a mosaic of proximal and distal tubule marker-positive cells reside side by side in the immature nephron. This suggests that each cell controls its own fate for becoming a proximal or distal tubule cell. In kidney injury models, the ratio of USAG-1 to BMP-7 expression decreased with kidney damage but increased after subsequent kidney regeneration. Our study suggests that USAG-1 expression in a kidney biopsy could be useful in predicting outcome.

Kidney International (2008) **73**, 181–191; doi:10.1038/sj.ki.5002626; published online 17 October 2007

KEYWORDS: kidney disease; differentiation; nephron segment

Correspondence: *M Yanagita, Graduate School of Medicine, Kyoto University, Yoshida-Konoe-cho, Kyoto, Japan 606-8501.*
E-mail: motoy@kuhp.kyoto-u.ac.jp

Received 6 April 2007; revised 3 August 2007; accepted 14 August 2007; published online 17 October 2007

Bone morphogenetic proteins (BMPs) are phylogenetically conserved signaling molecules that belong to the transforming growth factor-β superfamily.[1] Although these proteins were first identified by their capacity to promote endochondral bone formation, they are involved in the cascades of body patterning and morphogenesis. Furthermore, BMPs play important roles after birth in the pathophysiology of several diseases, including osteoporosis, arthritis, pulmonary hypertension, and kidney diseases.[2]

Bone morphogenetic protein-7 is a 35-kDa homodimeric protein, and kidney is the major site of BMP-7 synthesis during embryogenesis as well as in postnatal development. *BMP-7*-deficient mice die shortly after birth due to severe renal hypoplasia.[3,4] Mutant kidneys suffer gradual cessation of nephrogenesis, associated with a reduction in ureteric bud branching and loss of metanephric mesenchyme, indicating that BMP-7 is essential for survival and differentiation of mesenchymal cells in kidney development.[5] In postnatal life, many developmental features are recapitulated during renal injury, and BMP-7 has been shown to be important in both preservation of kidney function and resistance to injury. For example, BMP-7 inhibits tubular epithelial cell dedifferentiation,[6–10] mesenchyme transformation, and apoptosis stimulated by various renal injuries, and has an anti-inflammatory effect in models of both acute and chronic renal failure.[11]

The local activity of endogenous BMP-7 is controlled not only by the precise regulation of its expression, but also by certain classes of molecules that bind to BMP-7, acting as positive[12] or negative regulators of BMP-7 activity in the kidney.[2,13–15] BMP antagonists function through direct association with BMP, thus inhibiting the binding of BMP to its receptors, and define the boundaries of BMP activity.

Recently, we found that the product of uterine sensitization-associated gene-1 (USAG-1) acts as a kidney-specific BMP antagonist, and that USAG-1 binds to and inhibits the biological activity of BMP-7.[16] We further demonstrated that *USAG-1*-deficient mice are resistant to kidney injury, and that USAG-1 is the central negative regulator of BMP

function in the adult kidney.[17] Because the interaction between BMP-7 and USAG-1 seems to play critical roles in the kidney, we analyzed the balance between USAG-1 and BMP-7 expression in kidney injury and development, and demonstrated the reciprocal relationship between USAG-1 and BMP-7 expression in kidney injury and development. Close examination of USAG-1 expression in developing kidneys further provided a clue to proximal–distal differentiation mechanism of nephron by demonstrating the possibility that each single cell in an immature nephron controls its own fate to become proximal or distal tubule cell. In addition, USAG-1 expression in the kidney biopsy could be a powerful diagnostic tool to predict renal prognosis.

RESULTS

Generation of *USAG-1*$^{+/LacZ}$ knock-in mice

To facilitate the temporal and spatial analyses of USAG-1 expression, we generated in-frame *USAG-1*$^{+/LacZ}$ mice. In our previous work, the nuclear *lacZ* reporter gene that was knocked in[17] proved unsuitable for signal detection. In this work, the cytoplasmic *lacZ* reporter gene was used to replace the open reading frame of *USAG-1* and create a novel knock-in allele (Figure 1a). While *USAG-1*$^{+/LacZ}$ mice showed no overt defects, *USAG-1*$^{LacZ/LacZ}$ mice presented the same teeth phenotype as observed in the original *USAG-1* mutants.[17] *In situ* hybridization (ISH) of a *USAG-1* antisense probe to whole embryos at E9.5 and adult kidney specimen confirmed that lacZ staining in *USAG-1*$^{+/LacZ}$ mice reflected authentic *USAG-1* gene expression (Figure 1d).

USAG-1 is expressed in distal tubules and overlaps with BMP-7 in distal convoluted tubules

To further analyze the localization of USAG-1 expression in the kidney, we used several well-characterized segment markers. First, we clarified the segments in which well-known segment markers are expressed (Figure 2a). Tamm Horsfall glycoprotein (THP) was expressed in thick ascending limb. The calbindin D28K was expressed in distal convoluted tubules (DCTs) and connecting tubules (CTs). Using the antibody from Upstate, NaKATPase α-1 subunit was strongly expressed in thick ascending limb, DCT, and CT. AQP-1 was expressed in proximal tubules, descending thin limb, and possibly in ascending thin limb, while AQP-2 was expressed in the collecting ducts (CDs)[18] and CTs as reported.

Next, we analyzed the localization of USAG-1 in adult kidneys using these markers, and demonstrated that all the tubules expressing calbindin D28K or THP in the cortex expressed USAG-1 (Figure 2b and c). In the outer medulla, USAG-1 expression completely overlapped with THP (Figure 2d) and NaKATPase (Figure 2e), but not with AQP-2 (Figure 2f) or AQP-1 (Figure 2g). In addition, USAG-1 expression in the cortex did not overlap with AQP-2 (Figure 2f) or AQP-1 (Figure 2g), except for CTs, which were double positive for *lacZ* transcript and AQP-2 (data not shown). In the inner medulla, USAG-1 expression was not detected (Figure 1d). From these findings, we concluded that USAG-1 is predominantly expressed in the distal tubules, more specifically, in thick ascending limb, DCT, and CT in adult kidneys.

For comparison, the expression of BMP-7 was determined using *BMP-7*$^{+/LacZ}$ mice, and the tubules expressing calbindin D28K (Figure 2h) or AQP-2 (data not shown) were positive for *lacZ* transcript, indicating that BMP-7 is expressed in DCT, CT, and CD as previously reported (Figure 2a).[11]

USAG-1 emerges in developing nephrons and colocalizes with BMP-7 only in differentiated tubules

Next, we examined the expression of USAG-1 and BMP-7 in kidney development. The expression of USAG-1 increased toward the later stage of development, and peaked at E17.5, while BMP-7 was constantly expressed during kidney development and decreased at perinatal period (Figure 3a). As a result, the ratio between USAG-1 and BMP-7 expression increased significantly toward the later stage of development (Figure 3a). We also compared the ratio between other BMP antagonists and BMP-7, and demonstrated that USAG-1 is predominantly the major BMP antagonist during kidney development (Figure 3a). At E13.5, USAG-1 expression was almost absent (Figure 3b), while BMP-7 expression was intensely expressed in ureteric buds, adjacent metanephric mesenchyme, and part of comma-shaped body (Figure 3c). At E15.5, USAG-1 expression was still absent in the comma-shaped body, but was strongly detected in more differentiated tubular epithelial cells in the medulla, in a pattern similar to that of BMP-7, except for the expression in the podocyte layers of the developing glomeruli, where USAG-1 expression was absent (Figure 3b and c). Therefore, we conclude that USAG-1 emerges in developing nephrons and colocalizes with BMP-7 only in differentiated tubules (Figure 3d). We also examined the expression of several segmental markers in *USAG-1*-deficient kidney to determine whether the developmental process is modified; however, we could not observe any difference in the expression pattern of these markers (data not shown).

Mosaicism of proximal tubule marker-positive cell and distal tubule marker-positive cell in a single immature nephron

From E17.5 to the neonatal period, two patterns of USAG-1 expression were observed in the kidneys: a strong signal in distal tubules (Figure 3b, arrowheads) and a weak, patchy signal in the cortex (Figure 3b, arrows). To demonstrate that both signals were not due to endogenous β-galactosidase activity in the kidney, kidneys of wild-type mice were subjected to lacZ staining and incubated for the same period of time, but no signal was detected (Figure 3b).

We further analyzed the property of these signals with segment markers, and found that the strong signal in neonatal *USAG-1*$^{+/LacZ}$ kidneys colocalized with THP and NaKATPase (Figure 4a and b), but not with AQP-1 or AQP-2 (Figure 4c and d). Calbindin D28K was hardly detected in the

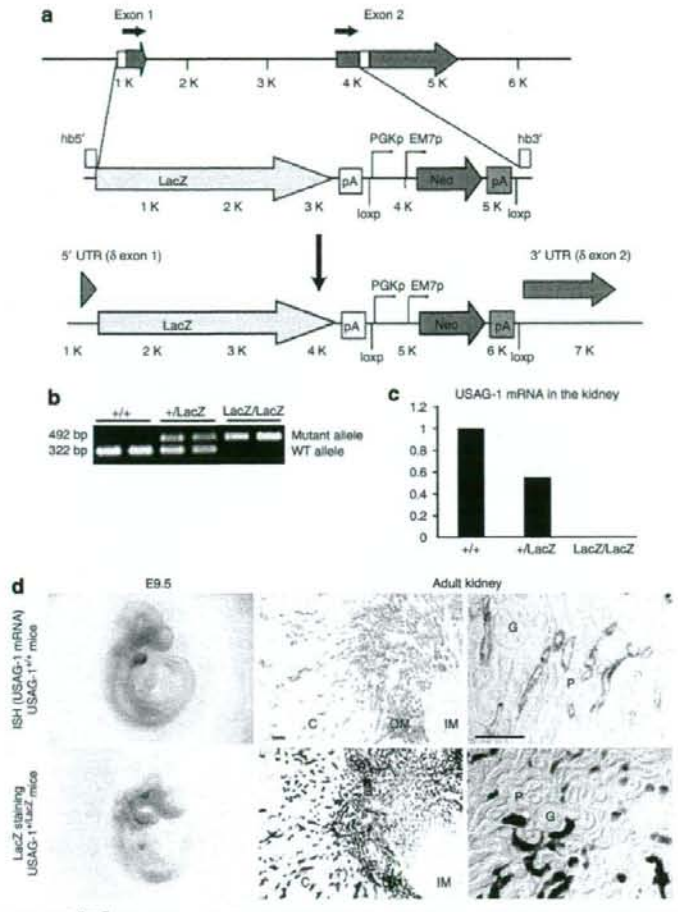

Figure 1 | Generation of USAG-1 $^{+/LacZ}$ knock-in mice by gene targeting. (**a**) Design of *Sostdc1* (gene symbol for *USAG-1*) null allele with concomitant replacement by LacZ. Light gray arrows depict the two exons; black arrows indicate the coding sequence. The homology boxes used for bacterial homologous recombination (BHR) are depicted as white (hb5′ and hb3′). The entire coding sequence of *Sostdc1* was replaced by LacZ/Neo, in a manner such that the initiating ATG of *Sostdc1* became the ATG of LacZ. The reporter open reading frame (ORF), LacZ, is followed by an SV40 polyadenylation signal and SV40-derived associated sequence[31] (purple boxes), whereas, the Neo ORF is followed by the mouse PGK polyadenylation signal and associated sequence[32] (yellow boxes). All of these elements are standard elements used by Velocigene.[29] The replacement afforded into the *Sostdc1* BAC by BHR is also translated in an identical manner into the mouse genome during targeting. Therefore, all the features shown above are also those present in the modified *Sostdc1* locus in the targeted embryonic stem (ES) cells. (**b**) PCR genotyping of *USAG-1* $^{+/+}$, *USAG-1* $^{+/LacZ}$, and *USAG-1* $^{LacZ/LacZ}$ littermates. (**c**) Real-time RT-PCR analysis of *USAG-1* mRNA in the kidneys of *USAG-1* $^{+/+}$, *USAG-1* $^{+/LacZ}$, and *USAG-1* $^{LacZ/LacZ}$ littermates. Expression of *USAG-1* was normalized to that of *GAPDH* and expressed relative to that in *USAG-1* $^{+/+}$ mice. (**d**) ISH of whole embryo and adult kidney section revealed a similar distribution of *USAG-1* mRNA and *lacZ* transcripts. C, cortex; OM, outer medulla; IM, inner medulla; P, proximal tubule; G, glomerulus. Bar = 100 μm.

immature nephron at this stage. On the other hand, only the weak, patchy signal, but not the strong signal, colocalized with the expression of the lectin-binding sites for Lotus Tetragonolobus Agglutnin (LTA) (Figure 4e), the marker for proximal tubules.[19] NDRG1, the cytoplasmic protein upregulated in several stress stimuli,[20] is known to be expressed in the proximal tubules and CDs in the kidney.[21] The weak, patchy signal of lacZ staining also colocalized with NDRG1 expression (Figure 4f), indicating that these tubules with weak, patchy signal of lacZ staining possess proximal tubule property, as well. AQP-1 was partially positive in the descending part of weak, patchy blue tubules (Figure 4d), possibly indicating that these tubules might have the characteristics of proximal tubules and thin limbs of Henle.

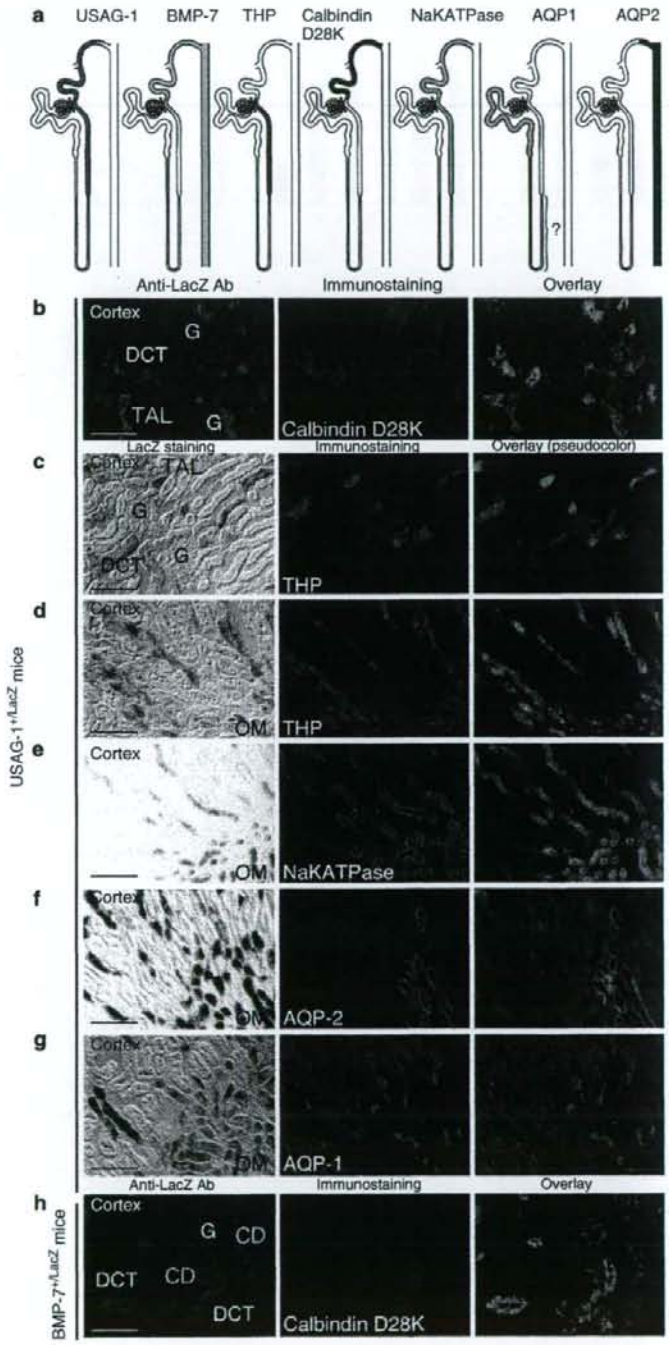
a
USAG-1
BMP-7
THP
Calbindin D28K
NaKATPase
AQP1
AQP2
?
Anti-LacZ Ab
Immunostaining
Overlay
b
Cortex
G
DCT
TAL
G
Calbindin D28K
LacZ staining
Immunostaining
Overlay (pseudocolor)
c
Cortex
TAL
G
DCT
G
THP
d
Cortex
OM
THP
e
Cortex
OM
NaKATPase
f
Cortex
OM
AQP-2
g
Cortex
OM
AQP-1
Anti-LacZ Ab
Immunostaining
Overlay
h
Cortex
G
CD
DCT
CD
DCT
Calbindin D28K
USAG-1+/LacZ mice
BMP-7+/LacZ mice

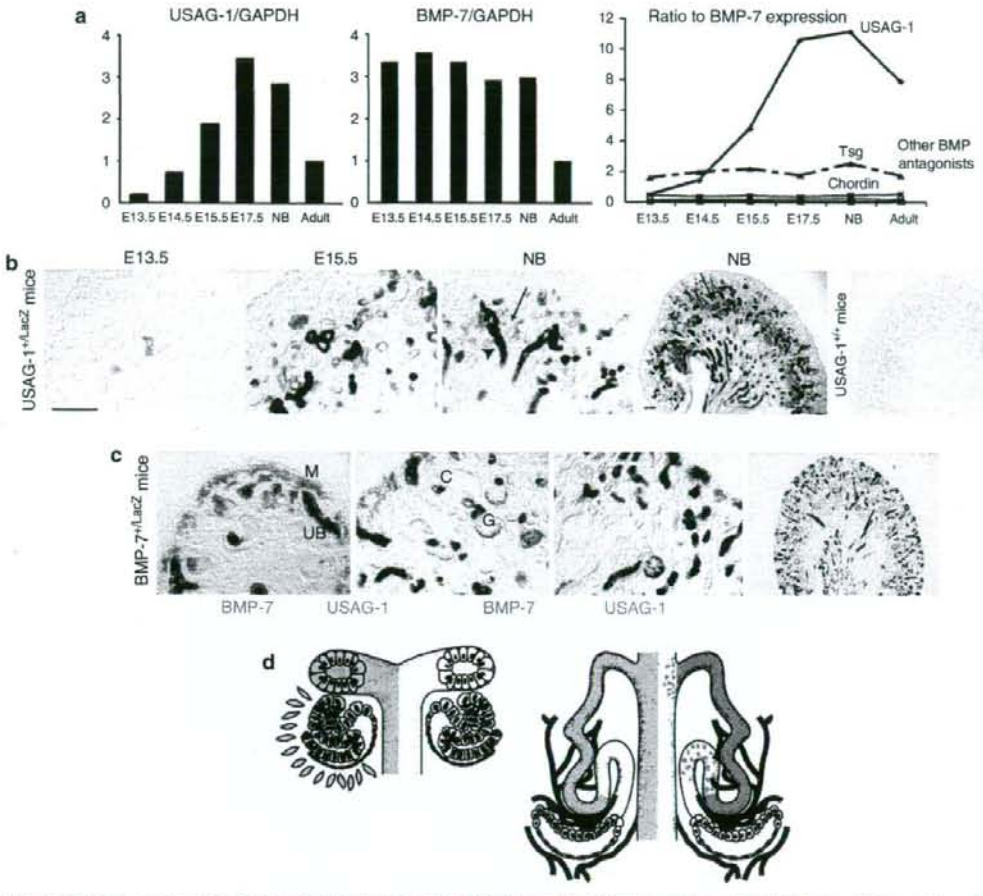

Figure 3 | USAG-1 emerged in developing nephrons and colocalized with BMP-7 in differentiated tubules. (**a**) Expression of USAG-1 and ratio of USAG-1/BMP-7 expression increased in kidney development. Metanephric kidneys from five to six embryos at indicated time points, and kidneys from seven neonates were collected and subjected to RNA extraction. Expression levels of USAG-1 and BMP-7 were normalized to the expression of GAPDH and expressed relative to the expression level in the adult kidney. The ratio of USAG-1 and other BMP antagonists to BMP-7 expression was determined as described (see Materials and Methods). (**b** and **c**) Localization of *lacZ* transcripts in developing *USAG-1*$^{+/LacZ}$ (**b**) and *BMP-7*$^{+/LacZ}$ (**c**) kidneys. Expression of *USAG-1/lacZ* transcripts did not emerge in immature nephrons, where BMP-7 facilitates differentiation, but was strong and overlapped with that of BMP-7 in the fully differentiated tubules (arrowheads). Besides, the strong signal of *USAG-1/lacZ* transcripts in distal tubules (arrowhead), a weak, patchy signal was observed in the neonatal kidneys (arrows). UB, ureteric bud; M, mesenchyme; C, comma-shaped body; G, glomerulus. Bar = 100 μm. (**d**) Schematic illustration demonstrating the expression of USAG-1 and BMP-7 during kidney development. USAG-1 expression was negative in the immature nephron, where BMP-7 was strongly expressed and promoted differentiation. USAG-1 expression emerged in more differentiated tubules and overlapped with that of BMP-7.

Figure 2 | USAG-1 and BMP-7 overlap in DCTs. (**a**) Schematic illustration demonstrating the expression of USAG-1, BMP-7, and other segment markers in the nephron. USAG-1 is expressed in thick ascending limb (TAL), DCTs, and in CTs, while BMP-7 is expressed in DCT, CT, and in CD. (**b**) Tubules positive for calbindin D28K are positive for *LacZ* transcripts in the kidneys of *USAG-1*$^{+/LacZ}$ mice. G, glomerulus. Bar = 100 μm. (**c**) Tubules positive for THP in the cortex are positive for *LacZ* transcripts in the kidneys of *USAG-1*$^{+/LacZ}$ mice. (**d**) Tubules positive for THP in the cortex and medulla are positive for *LacZ* transcripts in the kidneys of *USAG-1*$^{+/LacZ}$ mice. OM, outer medulla. (**e**) Tubules positive for NaKATPase in the cortex and medulla are positive for *LacZ* transcripts in the kidneys of *USAG-1*$^{+/LacZ}$ mice. (**f** and **g**) Tubules positive for AQP-2 (**f**) or AQP-1 (**g**) are negative for *LacZ* transcripts in the kidneys of *USAG-1*$^{+/LacZ}$ mice. (**h**) Tubules positive for calbindin D28K are positive for *LacZ* transcripts in the kidneys of *BMP-7*$^{+/LacZ}$ mice. *LacZ* transcripts in the kidneys of *BMP-7*$^{+/LacZ}$ mice are also positive in CD and podocyte in glomeruli.

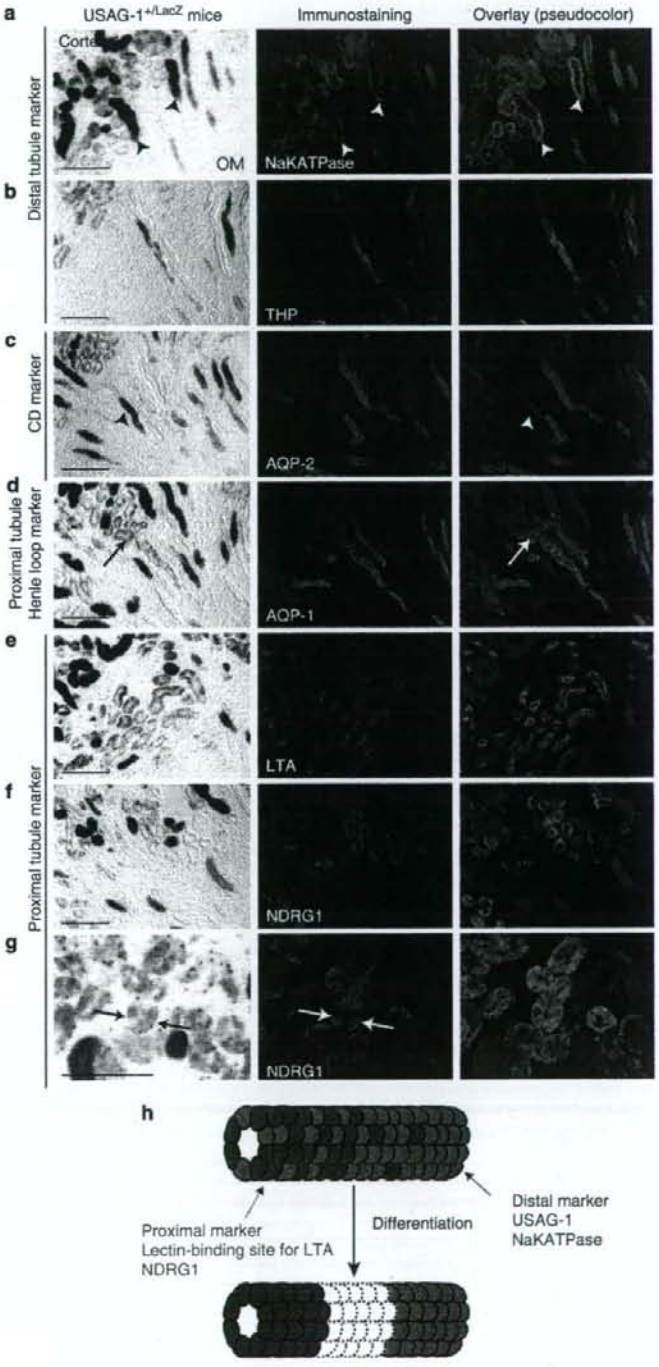
a
USAG-1+/LacZ mice
Immunostaining
Overlay (pseudocolor)
Distal tubule marker
Cortex
OM
NaKATPase
b
THP
c
CD marker
AQP-2
d
Proximal tubule
Henle loop marker
AQP-1
e
LTA
f
Proximal tubule marker
NDRG1
g
NDRG1
h
Differentiation
Distal marker
USAG-1
NaKATPase
Proximal marker
Lectin-binding site for LTA
NDRG1

Close examination of these tubules further clarified that the weak, patchy signal of lacZ staining and NDRG1 signals were not overlapping in a single cell, but were complementary in the single tubule (Figure 4g); therefore, the tubule in this area was made up of two types of epithelial cells: those with distal tubule property and those with proximal tubule property (Figure 4h). To exclude the possibility that lacZ staining quenches the fluorescence of other markers, immunostaining of the serial sections was performed and demonstrated similar results (data not shown).

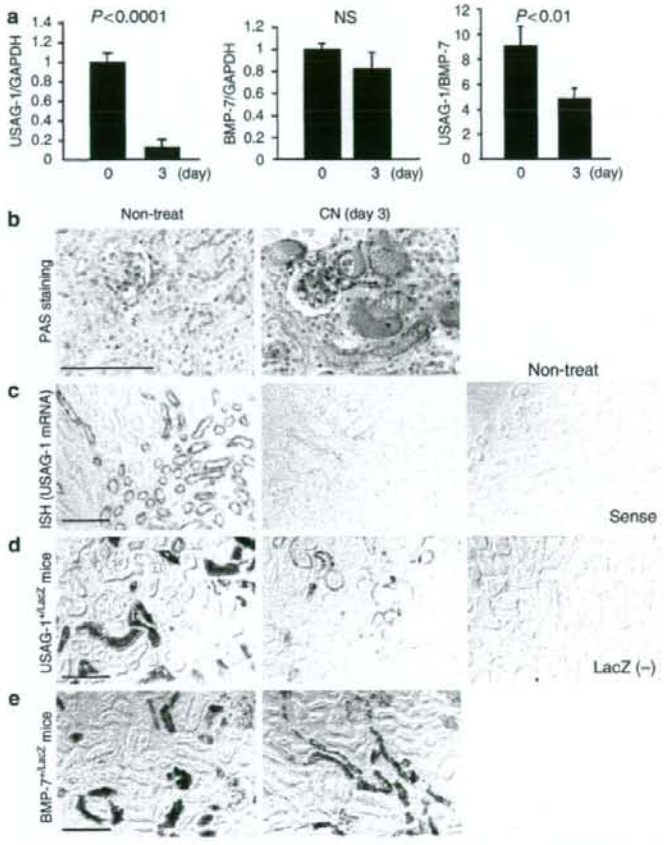

Figure 5 | Expression of USAG-1 decreased in tubular injury. (**a**) Expression of *USAG-1* mRNA decreased in acute tubular injury. Expression of USAG-1 and BMP-7 and the ratio between USAG-1 and BMP-7 expression during cisplatin nephrotoxicity (CN) were determined by real-time RT-PCR. Expression of USAG-1 and BMP-7 was normalized to that of GAPDH and expressed relative to that in mice on day 0. The ratio between USAG-1 and BMP-7 expression was determined by setting the standard curve with plasmids encoding each gene at various concentrations and analyzing the copy number of each gene contained in kidney cDNA (see Results). $N = 4$–6 for each experiment. (**b**–**e**) Representative histological findings (**b**), ISH of *USAG-1* mRNA (**c**), and lacZ staining of the *USAG-1*$^{+/LacZ}$ (**d**), and *BMP-7*$^{+/LacZ}$ (**e**) kidneys during CN. Bar = 100 μm.

Figure 4 | Mosaicism of proximal tubule marker-positive cell and distal tubule marker-positive cell in a single immature nephron. (**a**) Strong (arrowheads) and weak, patchy signal of *lacZ* transcripts in neonatal *USAG-1*$^{+/LacZ}$ kidneys colocalized with NaKATPase. Bar = 100 μm. (**b**) Strong signal of *lacZ* transcripts in neonatal *USAG-1*$^{+/LacZ}$ kidneys colocalized with THP. (**c**) *LacZ* transcripts in neonatal *USAG-1*$^{+/LacZ}$ kidneys did not colocalize with AQP-2. (**d**) AQP-1 was partially positive in the descending tubules with weak, patchy signal of *lacZ* transcripts (arrow). (**e**) Weak, patchy signal of *lacZ* transcripts colocalized with lectin-binding sites for Lotus Tetragonolobus Agglutnin (LTA). (**f**) Weak, patchy signal of *lacZ* transcripts colocalized with NDRG1. (**g**) Close examination of the overlapping areas demonstrated that the weak, patchy signal of *lacZ* transcripts (arrows) was not overlapping with NDRG1 expression, but was complementary in a single tubule. (**h**) Working hypothesis for proximal–distal differentiation mechanism of kidney tubules. Proximal tubule marker-positive cells (green) lie side by side with distal tubule marker-positive cells (red) in a single immature nephron. It is postulated that each single cell possesses its cell fate to become proximal or distal tubular cell.

The ratio between USAG-1 and BMP-7 expression was reduced in tubular injury and increased in tubular regeneration

We also examined the expression of USAG-1 and BMP-7 in kidney injury. Administration of cisplatin causes acute tubular necrosis and apoptosis, leading to deterioration of renal function. USAG-1 but not BMP-7 mRNA in the kidney decreased at day 3 of cisplatin nephrotoxicity (Figure 5a). ISH and lacZ staining demonstrated that USAG-1 expression was significantly reduced at day 3 of cisplatin nephrotoxicity, while the lacZ staining in *BMP-7*$^{+/LacZ}$ mice was maintained (Figure 5c–e). At day 0 of cisplatin nephrotoxicity, the expression level of USAG-1 was much higher than that of BMP-7, but at day 3, the ratio between USAG-1 and BMP-7 expression was significantly decreased, indicating that the reduction of USAG-1 expression was more prominent than that of BMP-7.

Next, we examined the expression of USAG-1 in the kidney regeneration. Administration of folic acid (FA) to mice causes intratubular crystallization, which results in dilatation and degeneration of tubules, leading to transient acute renal failure[22] (Figure 6a). In contrast to the cisplatin nephrotoxicity model, damaged tubular epithelial cells proliferate and regenerate after several days, and renal function returns to normal by day 14 (Figure 6a). Expression of USAG-1 in this model decreased during tubular epithelial damage (day 1), but increased markedly during proliferation and regeneration of tubular epithelial cells (days 7–10), and

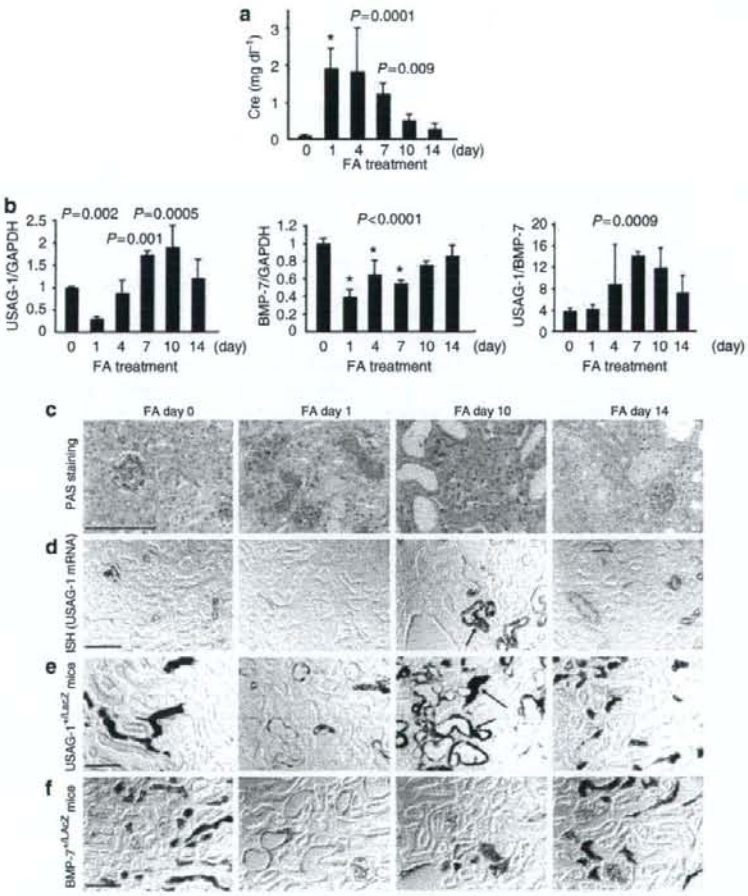

Figure 6 | Expression of USAG-1 increased in tubular regeneration. (**a**) Time course of serum creatinine level in FA nephrotoxicity model. (**b**) Expression of USAG-1 and BMP-7 and the ratio between USAG-1 and BMP-7 expression after FA treatment. $N = 4$–6 for each experiment. (**c**–**f**) Representative histological findings (**c**), ISH of USAG-1 mRNA (**d**), and lacZ staining of the *USAG-1*$^{+/LacZ}$ (**e**) and *BMP-7*$^{+/LacZ}$ kidneys (**f**) after FA treatment. Bar = 100 μm. USAG-1 was strongly detected in the irregularly lined regenerating epithelial cells (**d** and **e**; arrows).

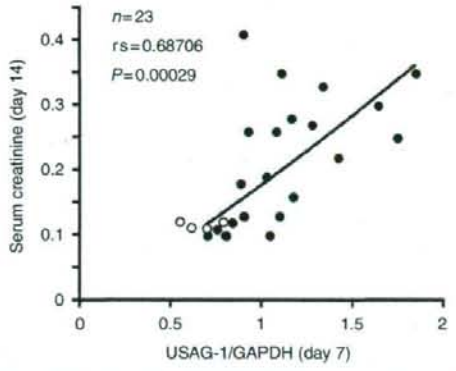

Figure 7 | USAG-1 as a diagnostic marker for renal prognosis. A significant correlation is observed between *USAG-1* expression in kidney biopsy sample at day 7 and serum creatinine at day 14 in FA nephrotoxicity (closed circle, $N = 23$). Open circles indicate control kidneys without FA nephrotoxicity ($N = 4$).

returned to the basal level when redifferentiation of tubular epithelial cells was completed (day 14), while the expression of BMP-7 increased gradually after the initial dip at day 1 (Figure 6b). ISH and lacZ staining demonstrated that USAG-1 was strongly detected in the irregularly lined regenerating tubular epithelial cells at day 10 (Figure 6d and e, arrows), which might account for the increase in USAG-1 expression at this time point (Figure 6b). The ratio between USAG-1 and BMP-7 expression was significantly increased during the regeneration phase (Figure 6b). We also compared the ratio between other BMP antagonists and BMP-7 in both kidney disease models, and demonstrated that USAG-1 is predominantly the major BMP antagonist during kidney injury (Figure S1).

USAG-1 as a predictive marker for renal prognosis

Because USAG-1 is a negative regulator of the renoprotective action of BMP-7, we postulated that high expression of USAG-1 in the kidney biopsy might predict poor renal prognosis.

Because regenerating tubules and damaged tubules are observed in the regenerating period (days 7–10) of FA nephrotoxicity and might mimic the situation in the clinical kidney biopsy specimen, we utilized the model and performed kidney biopsy at day 7 and examined renal function at day 14. Interestingly, the expression of USAG-1 in kidney biopsy at day 7 correlated significantly with renal function at day 14 (Figure 7), indicating the possibility that USAG-1 could be a predictive marker of renal prognosis. We also performed renal biopsies at days 1 and 10. As shown in Figure S2, USAG-1 expression at day 10 ($N = 4$, regenerating period) correlated well with future renal function at day 14, while USAG-1 expression at day 1 ($N = 8$, tubular damage period) did not. Therefore, we conclude that USAG-1 expression correlated well with future renal function when tubular regeneration is observed.

DISCUSSION

USAG-1 colocalizes with BMP-7 only in differentiated tubules in developing kidney

During kidney development, BMP-7, made by both metanephric mesenchyme and tubular epithelial cells (Figure 3c), is a facilitator of ureteric bud branching at low concentrations, but an inhibitor of branching at high concentrations.[23] The discrepancy is a part of a feedback mechanism that allows ureteric buds to branch into 'unpopulated' areas of mesenchyme, but not into areas already populated by nephrons and other bud branches. USAG-1 expression did not emerge in immature nephrons where BMP-7 facilitates differentiation, but was strongly expressed and overlapped with BMP-7 in fully differentiated tubules (Figure 3b and c). We also demonstrated that USAG-1 expression is lower than that of BMP-7 at E13.5, is comparable at E14.5 and E15.5, and is much higher at E17.5 and in newborns (Figure 3a). In addition, USAG-1 is the major BMP antagonist during kidney development (Figure 3a). These data support the idea that USAG-1 might function as a feedback mechanism for BMP-7 activity during kidney development. However, no developmental abnormality was observed in the kidney of *USAG-1*-deficient mice,[17] and some redundant factor might overcome the lack of USAG-1 in the kidney of *USAG-1*-deficient mice during development. Twisted gastrulation is one candidate for the redundancy, because the expression pattern is similar to that of USAG-1 and the expression level is the second highest among BMP antagonists to USAG-1 (Figure 3a).

USAG-1 expression gives an insight into proximal-distal differentiation mechanism of immature nephron

In spite of that USAG-1 expression was confined to distal tubules in adult kidney, weak, patchy expression of USAG-1 in neonatal kidneys colocalized with proximal tubular markers, such as lectin-binding site for Lotus Tetragonolobus and NDRG1 in the cortex. NaKATPase, another distal tubule marker, also colocalized with proximal tubular markers in the area (data not shown). AQP-1 was partially positive in the descending part of weak, patchy blue tubules, possibly indicating that these tubules might also have the property of proximal tubules and thin limbs of Henle. Close examination of the area double positive for proximal and distal markers further demonstrated that each single cell is not double positive for these two markers, but two types of cells positive for each marker intermingled with each other in a single tubule (Figure 4g and h). Little is known about the mechanism how uniform mesenchymal cells differentiate to a variety of cells, including glomerular epithelial cells, proximal tubular cells, and distal tubular cells, along the proximal–distal axis.[24] There has been a controversy between the following two hypotheses: gradient of growth factors brings the proximal–distal differentiation, or cell fate is determined for each cell. Recent studies revealed critical roles of Notch in the determination of proximal tubule cells and the fates of podocytes.[25–27] Our data might support the cell fate

hypothesis because the proximal tubule marker-positive cell lies side by side with the distal tubule marker-positive cell in a single tubule (Figure 4g and h), and such chimeric tubule could not be made by the gradient of growth factors. From these findings, we postulate that each single cell possesses its cell fate to become proximal tubular cell or distal tubular cell. Further study is needed to clarify how these chimeric tubules differentiate to mature tubules (Figure 4h). Interestingly, all tubule epithelial cells positive for proximal tubule marker reside in the chimeric tubules in neonatal kidney, while some distal tubule marker-positive cells reside outside the area and are terminally differentiated (Figure 4a and c, arrowheads, H), indicating the possible sequence of differentiation.

USAG-1 expression decreases in tubular injury and increases in tubular regeneration

In the adult kidney, we demonstrated that the expression of USAG-1 colocalized with BMP-7 in DCTs (Figure 2a) and decreased in acute tubular injury (Figure 5). The reduction of USAG-1 expression in renal injury is not simply due to loss of tubular epithelial cells, because USAG-1 expression decreased rapidly in the very early stage of diseases, when morphological changes of tubular epithelial cells were not obvious (data not shown).

During the recovery from renal failure, regeneration of tubular epithelial cells occurs via proliferation and redifferentiation of surviving renal cells.[28] In the FA model, USAG-1 expression decreased during tubular injury, increased markedly during the regeneration of surviving cells, and returned to the basal level after redifferentiation was completed (Figure 6b). In contrast, the expression of BMP-7 increased gradually to the basal level after the initial dip during tubular injury (Figure 6b), resulting in a significant increase in the ratio between USAG-1 and BMP-7 during regeneration. Further examination with *USAG-1*-deficient mice is needed to clarify the role of USAG-1 in the regeneration of kidney injury.

USAG-1 could be a diagnostic marker for renal prognosis

In the clinical setting, prediction of renal prognosis is difficult even with histological examination, because damaged tubules and regenerating tubules are mixed in the single specimen, and are indistinguishable by morphology. Because USAG-1 is a negative regulator of the renoprotective action of BMP-7, we postulated that high expression of USAG-1 during kidney diseases might be a sign of poor renal prognosis. Because the coexistence of regenerating tubules and damaged tubules in FA nephrotoxicity model resembles the situation of renal biopsy in patients, we utilized the model and proved that high expression of USAG-1 in kidney biopsy in regenerating period correlated well with poor renal prognosis. Because the expression of USAG-1 is confined to the kidney, serum concentration of USAG-1 might reflect the renal expression level of USAG-1. In that case, blood test for USAG-1 concentration might be enough to predict renal prognosis and is suitable for health examination.

MATERIALS AND METHODS

Derivation of USAG-1/LacZ mice

To generate a null allele of *Sostdc1* (gene symbol for *USAG-1*), the coding sequence was replaced with the coding sequence of the marker gene LacZ, using Velocigene technology, essentially as described (Figure 1a).[29] PCR genotyping was performed in all subsequent studies to allow specific detection of the genotype (Figure 1b). The sequences of the primers used were as follows: primer A, CCTTCTCTGTGTTTTCACTCCG; primer B, TGATTCAGGGTGCTG TTGC; and lacZRev, CCGTAATGGGATAGGTCACG.

β-gal staining and *in situ* hybridization

β-gal staining and ISH were performed as described previously.[17,29] Probe for ISH was designed to contain the open reading frame with the following length and GC content: USAG-1, 1.0 kbp (GC 52.6%). Hybridization was detected using an anti-DIG AP conjugate (Roche, Basel, Switzerland) and NBT/BCIP solution (Roche).

Histological studies and immunostaining

The kidneys were fixed in Carnoy's solution, embedded in paraffin, and sections (4 μm thick) were stained with periodic acid-Schiff for routine histological examination. Frozen sections of the kidneys and primary kidney tubular cells were immunostained as previously described.[30] Reagents utilized were anti-NaKATPase α-1 antibody (Ab) (Upstate, Billerica, MA, USA), anti-calbindin D28K (Sigma, St Louis, MO, USA), anti-Tamm Horsfall Protein Ab (Biomedical Technologies Inc.), anti-aquaporin 1 Ab (Chemicon, Temecula, CA, USA), anti-aquaporin 2 Ab (Calbiochem, Darmstadt, Germany), FITC-conjugated lotus tetragonolobus agglutinin (LTA) (Sigma), anti-LacZ Ab (Cappel, Solon, OH, USA), and anti-NDRG1 Ab.[20] For double staining, immunostaining was performed before β-gal staining, to avoid the possibility that the deposition of X-gal interferes with antibody binding to the antigen.

Quantification of mRNA by real-time RT-PCR

Real-time reverse transcription (RT)–PCR was performed as described previously.[17] Specific primers were designed using Primer Express software (Applied Biosystems, Foster City, CA, USA). To compare the expression levels of different genes, we used modified real-time PCR by setting the standard curves with plasmids encoding each gene at various concentrations, and analyzed the copy number of each gene contained in kidney cDNA as previously described.[17] Serially diluted cDNA or plasmids were used to generate the standard curve for each primer, and the PCR conditions were as follows: 50 °C for 2 min, 95 °C for 10 min, then 95 °C for 15 s, and 60 °C for 1 min for 40 cycles.

Kidney disease models

Cisplatin nephrotoxicity was caused as described previously.[17] Briefly, cisplatin (20 mg kg^{-1}, Sigma-Aldrich) was administered by a single intraperitoneal injection to 8-week-old female C57BL/6J mice (SLC Japan, Shizuoka, Japan). FA nephrotoxicity was caused by a single intraperitoneal injection of FA (250 mg kg^{-1}, Sigma-Aldrich) in 0.15 M $NaHCO_3$ to 11-week-old male C57BL/6J mice. The kidneys were collected at days 0, 1, 4, 10, and 14, with at least three animals at each time point.

Animal use

All mice were housed in specific pathogen-free conditions. All animal experiments were performed in accordance with the institutional guidelines as well as the National Institutes of Health (NIH) guidelines.

Statistical analysis

All assays were performed in triplicate. Data were presented as mean ± s.d. Statistical significance was assessed by analysis of variance, followed by Fisher's protected LSD *post hoc* test. Correlation was determined by Spearman's correlation analysis.

ACKNOWLEDGMENTS

We thank Drs Y Nabeshima, E Nishi, and T Nakamura for valuable comments and discussion; S Tahara and A Yoshioka for experiments not included in the manuscript; and A Hosotani for technical assistance. This study was supported by grants-in-aid from the Ministry of Education, Culture, Science, Sports, and Technology of Japan (177090551); a Center of Excellence grant from the Ministry of Education, Culture, Science, Sports, and Technology of Japan; a research grant for health sciences from the Japanese Ministry of Health, Labor and Welfare; a grant from the Astellas Foundation for Research on Metabolic Disorders; a grant from the Novartis Foundation for the promotion of science; a grant from Kato Memorial Trust for Nambyo Research; a grant from Hayashi Memorial Foundation for Female Natural Scientists; and a grant from Japan Foundation for Applied Enzymology.

SUPPLEMENTARY MATERIAL

Figure S1. Relative expression of USAG-1 and other BMP antagonists to BMP-7 in kidney disease models.

Figure S2. Significant correlation was observed between *USAG-1* expression and future serum creatinine (day 14) in case that kidney biopsy was performed at day 10 but not at day 1 in folic acid nephrotoxicity (closed circles).

REFERENCES

1. Reddi AH. Bone morphogenetic proteins and skeletal development: the kidney-bone connection. *Pediatr Nephrol* 2000; **14**: 598–601.
2. Massague J, Chen YG. Controlling TGF-beta signaling. *Genes Dev* 2000; **14**: 627–644.
3. Dudley AT, Lyons KM, Robertson EJ. A requirement for bone morphogenetic protein-7 during development of the mammalian kidney and eye. *Genes Dev* 1995; **9**: 2795–2807.
4. Luo G, Hofmann C, Bronckers AL *et al.* BMP-7 is an inducer of nephrogenesis, and is also required for eye development and skeletal patterning. *Genes Dev* 1995; **9**: 2808–2820.
5. Dudley AT, Robertson EJ. Overlapping expression domains of bone morphogenetic protein family members potentially account for limited tissue defects in BMP7 deficient embryos. *Dev Dyn* 1997; **208**: 349–362.
6. Kalluri R, Neilson EG. Epithelial-mesenchymal transition and its implications for fibrosis. *J Clin Invest* 2003; **112**: 1776–1784.
7. Zeisberg M, Hanai J, Sugimoto H *et al.* BMP-7 counteracts TGF-beta1-induced epithelial-to-mesenchymal transition and reverses chronic renal injury. *Nat Med* 2003; **9**: 964–968.
8. Zeisberg M, Shah AA, Kalluri R. Bone morphogenic protein-7 induces mesenchymal to epithelial transition in adult renal fibroblasts and facilitates regeneration of injured kidney. *J Biol Chem* 2005; **280**: 8094–8100.
9. Wang S, Chen Q, Simon TC *et al.* Bone morphogenic protein-7 (BMP-7), a novel therapy for diabetic nephropathy. *Kidney Int* 2003; **63**: 2037–2049.
10. Wang S, de Caestecker M, Kopp J *et al.* Renal bone morphogenetic protein-7 protects against diabetic nephropathy. *J Am Soc Nephrol* 2006; **17**: 2504–2512.
11. Gould SE, Day M, Jones SS *et al.* BMP-7 regulates chemokine, cytokine, and hemodynamic gene expression in proximal tubule cells. *Kidney Int* 2002; **61**: 51–60.
12. Lin J, Patel SR, Cheng X *et al.* Kielin/chordin-like protein, a novel enhancer of BMP signaling, attenuates renal fibrotic disease. *Nat Med* 2005; **11**: 387–393.
13. Reddi AH. Interplay between bone morphogenetic proteins and cognate binding proteins in bone and cartilage development: noggin, chordin and DAN. *Arthritis Res* 2001; **3**: 1–5.
14. Yanagita M. BMP antagonists: their roles in development and involvement in pathophysiology. *Cytokine Growth Factor Rev* 2005; **16**: 309–317.
15. Yanagita M. Modulator of bone morphogenetic protein activity in the progression of kidney diseases. *Kidney Int* 2006; **70**: 989–993.
16. Yanagita M, Oka M, Watabe T *et al.* USAG-1: a bone morphogenetic protein antagonist abundantly expressed in the kidney. *Biochem Biophys Res Commun* 2004; **316**: 490–500.
17. Yanagita M, Okuda T, Endo S *et al.* Uterine sensitization-associated gene-1 (USAG-1), a novel BMP antagonist expressed in the kidney, accelerates tubular injury. *J Clin Invest* 2006; **116**: 70–79.
18. Sasaki S, Fushimi K, Saito H *et al.* Cloning, characterization, and chromosomal mapping of human aquaporin of collecting duct. *J Clin Invest* 1994; **93**: 1250–1256.
19. Cho EA, Patterson LT, Brookhiser WT *et al.* Differential expression and function of cadherin-6 during renal epithelium development. *Development* 1998; **125**: 803–812.
20. Okuda T, Higashi Y, Kokame K *et al.* Ndrg1-deficient mice exhibit a progressive demyelinating disorder of peripheral nerves. *Mol Cell Biol* 2004; **24**: 3949–3956.
21. Wakisaka Y, Furuta A, Masuda K *et al.* Cellular distribution of NDRG1 protein in the rat kidney and brain during normal postnatal development. *J Histochem Cytochem* 2003; **51**: 1515–1525.
22. Long DA, Woolf AS, Suda T *et al.* Increased renal angiopoietin-1 expression in folic acid-induced nephrotoxicity in mice. *J Am Soc Nephrol* 2001; **12**: 2721–2731.
23. Gupta IR, Piscione TD, Grisaru S *et al.* Protein kinase A is a negative regulator of renal branching morphogenesis and modulates inhibitory and stimulatory bone morphogenetic proteins. *J Biol Chem* 1999; **274**: 26305–26314.
24. Dressler GR. The cellular basis of kidney development. *Annu Rev Cell Dev Biol* 2006; **22**: 509–529.
25. Cheng HT, Kopan R. The role of Notch signaling in specification of podocyte and proximal tubules within the developing mouse kidney. *Kidney Int* 2005; **68**: 1951–1952.
26. Chen L, Al-Awqati Q. Segmental expression of Notch and Hairy genes in nephrogenesis. *Am J Physiol Renal Physiol* 2005; **288**: F939–F952.
27. McLaughlin KA, Rones MS, Mercola M. Notch regulates cell fate in the developing pronephros. *Dev Biol* 2000; **227**: 567–580.
28. Thadhani R, Pascual M, Bonventre JV. Acute renal failure. *N Engl J Med* 1996; **334**: 1448–1460.
29. Valenzuela DM, Murphy AJ, Frendewey D *et al.* High-throughput engineering of the mouse genome coupled with high-resolution expression analysis. *Nat Biotechnol* 2003; **21**: 652–659.
30. Yanagita M, Arai H, Ishii K *et al.* Gas6 regulates mesangial cell proliferation through Axl in experimental glomerulonephritis. *Am J Pathol* 2001; **158**: 1423–1432.
31. Thimmappaya B, Zain BS, Dhar R *et al.* Nucleotide sequence of DNA template for the 3′ ends of SV40 mRNA. II. The sequence of the DNA fragment *Eco*RII-F and a part of *Eco*RII-H. *J Biol Chem* 1978; **253**: 1613–1618.
32. Adra CN, Boer PH, McBurney MW. Cloning and expression of the mouse pgk-1 gene and the nucleotide sequence of its promoter. *Gene* 1987; **60**: 65–74.